Photoacoustics 36 (2024) 100594

Contents lists available at ScienceDirect

Photoacoustics

journal homepage: www.elsevier.com/locate/pacs

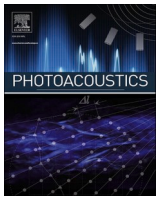

Mid-infrared all-fiber light-induced thermoelastic spectroscopy sensor based on hollow-core anti-resonant fiber

Weipeng Chen [a,b], Shunda Qiao [a,b], Ying He [a,b,*], Jie Zhu [c], Kang Wang [c], Lei Qi [d,**], Sheng Zhou [e], Limin Xiao [c,**], Yufei Ma [a,b,*]

[a] National Key Laboratory of Science and Technology on Tunable Laser, Harbin Institute of Technology, Harbin 150001, China
[b] Zhengzhou Research Institute, Harbin Institute of Technology, Zhengzhou 450000, China
[c] Advanced Fiber Devices and Systems Group, Key Laboratory of Micro and Nano Photonic Structures (MoE), Key Laboratory for Information Science of Electromagnetic Waves (MoE), Shanghai Engineering Research Center of Ultra-Precision Optical Manufacturing, School of Information Science and Technology, Fudan University, Shanghai, China
[d] Beijing Institute of Spacecraft Environment Engineering, Beijing 100094, China
[e] Laser Spectroscopy and Sensing Laboratory, Anhui University, Hefei 230601, China

ARTICLE INFO

Keywords:
Mid-infrared
All-fiber
Light-induced thermoelastic spectroscopy
Hollow-core anti-resonant fiber

ABSTRACT

In this article, a mid-infrared all-fiber light-induced thermoelastic spectroscopy (LITES) sensor based on a hollow-core anti-resonant fiber (HC-ARF) was reported for the first time. The HC-ARF was applied as a light transmission medium and gas chamber. The constructed all-fiber structure has merits of low loss, easy optical alignment, good system stability, reduced sensor size and cost. The mid-infrared transmission structure can be utilized to target the strongest gas absorption lines. The reversely-tapered SM1950 fiber and the HC-ARF were spatially butt-coupled with a V-shaped groove between the two fibers to facilitate gas entry. Carbon monoxide (CO) with an absorption line at 4291.50 cm^{-1} (2.33 μm) was chosen as the target gas to verify the sensing performance. The experimental results showed that the all-fiber LITES sensor based on HC-ARF had an excellent linear response to CO concentration. Allan deviation analysis indicated that the system had excellent long-term stability. A minimum detection limit (MDL) of 3.85 ppm can be obtained when the average time was 100 s

1. Introduction

Gas sensing technology is widely used in industrial process control, medical diagnostics, combustion diagnostics and many other fields due to its ability to systematically monitor, analyze and track changes in gas content and composition [1–13]. Laser absorption spectroscopy (LAS) is based on the "fingerprint" absorption spectrum characteristics of gas molecules, which retrieves gas concentration by measuring parameters related to the spectral characteristics of the measured gas [14–18]. Consequently, it offers the benefits of strong selectivity, high sensitivity and on line measurement [19–22]. As early as 2002, a quartz tuning fork (QTF) was applied in LAS technology, which is called quartz enhanced photoacoustic spectroscopy (QEPAS) technology [23]. In QEPAS, a QTF is used instead of a microphone as an acoustic detection element. Compared to microphone, QTF has a very narrow response bandwidth, which means it can minimize the environmental noise [24–27]. Simultaneously, QTF has advantages such as low cost, small size, and high quality factor (Q-factor), which reduces the cost of the sensor and improves its detection performance [28–31]. However, QEPAS is a contact measurement method since the QTF must be put in a gas chamber [32,33]. As a result, it cannot be used to detect corrosive gasses such as hydrogen chloride (HCl) and hydrogen sulfide (H_2S). The above limitation was overcome in 2018 by light-induced thermoelastic spectroscopy (LITES) [34]. In LITES, firstly the laser beam hit on a QTF's surface after passing through a gas chamber containing the tested gas. The laser energy is absorbed by the QTF, which transforms the heat energy into mechanical motion. Lastly, mechanical energy is further transformed into electrical signals due to quartz's piezoelectric effect [35–39]. Consequently, in LITES, there is no need to place the QTF in the gas chamber, so it is a non-contact measurement method. Meanwhile, LITES technology has the advantages of wide detection band, high sensitivity and strong noise immunity, and it is widely used in the gas

* Corresponding authors at: National Key Laboratory of Science and Technology on Tunable Laser, Harbin Institute of Technology, Harbin 150001, China.
** Corresponding authors.
E-mail addresses: hearkenyi@163.com (Y. He), qilei511@126.com (L. Qi), liminxiao@fudan.edu.cn (L. Xiao), mayufei@hit.edu.cn (Y. Ma).

https://doi.org/10.1016/j.pacs.2024.100594
Received 29 November 2023; Received in revised form 5 February 2024; Accepted 7 February 2024
Available online 9 February 2024

sensing field [40–43].

According to Beer-Lambert law, LITES signal value is positively correlated with the gas absorption path. In conventional LITES, a multi-pass cell (MPC) is typically applied to increase the gas absorption path [44,45]. Nevertheless, MPC has the disadvantages of large size, heavy weight and difficult to integrate, which makes it difficult to meet the needs of miniaturization and integration of sensors. To address the above challenges, an alternative solution is to use hollow-core fiber (HCF) for gas sensing. In 2020, Hu et al. built a near-infrared all fiber system using a hollow-core photonic crystal fiber (HC-PCF) [46]. The all fiber structure has advantages such as lower loss, easier optical alignment, reduced sensor size and cost [47]. But the detection performance of the system is limited by the internal mode interference of HC-PCF [48]. In 2022, Ma et al. constructed a near-infrared gas sensing system based on a lens set using a hollow-core anti-resonant fiber (HC-ARF) [49]. The special circular structure in HC-ARF has a good suppression effect on mode interference noise in fiber [50–52]. However, the use of lenses has negative effects such as increased system losses and size, and reduced system stability. Moreover, both of the above works investigated the sensing performance of HCF in near-infrared. For most gas molecules, they have stronger absorption coefficients in the mid-infrared spectral region than in the near infrared region. Therefore, extending gas sensing research to the mid-infrared region is of great significance for improving the detection performance.

In this manuscript, a mid-infrared all-fiber LITES sensor using a HC-ARF was reported for the first time. Instead of MPC, HC-ARF was adopted as a light transmission medium and gas chamber to improve the system stability and reduce system volume. Compared to the usually used HCF in all-fiber structure, the special circular structure in HC-ARF has a good suppression effect on mode interference noise in fiber. The laser that excites QTF vibration was guided directly from the end of the HC-ARF to the surface of the QTF, rather than focusing with a lens. The built all-fiber structure has many advantages such as low loss, easy optical alignment, robust system stability, reduced sensor size and cost. The mid-infrared transmission structure can be utilized to target the strongest gas absorption lines due to the fact that the fundamental gas absorption band is located in the mid-infrared. The reversely-tapered SM1950 fiber and the HC-ARF were spatially butt-coupled with a V-shaped groove between the two fibers to facilitate gas entry. Carbon monoxide (CO) with an absorption line at 4291.50 cm^{-1} (2.33 μm) was chosen as the target gas to verify the sensing characteristics. A continuous wave (CW) distributed feedback (DFB) diode laser with an output wavelength of 2.3 μm was selected as the system excitation source.

2. Experimental setup

In this study, a HC-ARF with a length of 55 cm was used. Fig. 1(a) displays the cross-section image of the HC-ARF, as captured by the scanning electron microscope (SEM). The HC-ARF has an air core structure, with six sets of discrete capillaries or nested capillaries forming a negative curvature core wall. This double-layer structure can reduce the transmission loss of fiber. The wall's thickness of the cladding capillary decides the order of wavelength, which can effectively suppress the coupling between the core mode and the cladding mode, and thus restricts most of the light to propagate in the air core. This feature greatly overcomes the influence of the substrate material, and significantly reduces the material loss. The maximum distance between two capillaries is 33 μm. Fig. 1(b) shows the transmission spectrum of the used HC-ARF in the range of 1.5 μm to 2.5 μm, which is limited by the spectral analyzer. It can be seen that the fiber at the selected wavelength (2.33 μm) in this experiment has a loss of 9.4 dB.

The configuration of all-fiber LITES sensor based on HC-ARF is shown in Fig. 2. Wavelength modulation spectroscopy (WMS) and second-harmonic (2*f*) demodulation technology were applied in the experiments. A low-frequency sawtooth wave generated by a signal generator to scan the CO absorption line and a high-frequency sine wave produced by a lock-in amplifier to modulate the laser wavelength were combined together to inject into the diode laser with an output wavelength of 2.3 μm. The laser beam was coupled into a single-mode fiber (SM1950) through a flange plate. In order to ensure the laser beam and CO molecules enter the HC-ARF smoothly, the reversely-tapered SM1950 fiber [53,54] and the HC-ARF were spatially butt-coupled with a gap in the experiment. The coupling loss was 2.2 dB. The spatial coupling region was placed in a 3D-printed gas chamber. After the laser and CO molecules fully reacted in the HC-ARF, the laser was guided out from the HC-ARF tip directly to the root of QTF, where it had the maximum thermoelastic effect. The QTF absorbed optical energy and then produced thermoelastic deformation, which was further converted into an electrical signal according to the piezoelectric effect of quartz. The electrical signal was demodulated by a lock-in amplifier whose integration time and detection bandwidth were 200 ms and 405.4 mHz, respectively. Two mass flow controllers were used to control the flow rate of CO and pure nitrogen (N_2) to obtain different concentrations of CO. The light spots at the tail fiber of the diode laser and at the end of the HC-ARF were captured using a beam quality analyzer, both of which exhibited a Gaussian distribution, indicating that HC-ARF had a good inhibitory effect on mode noise.

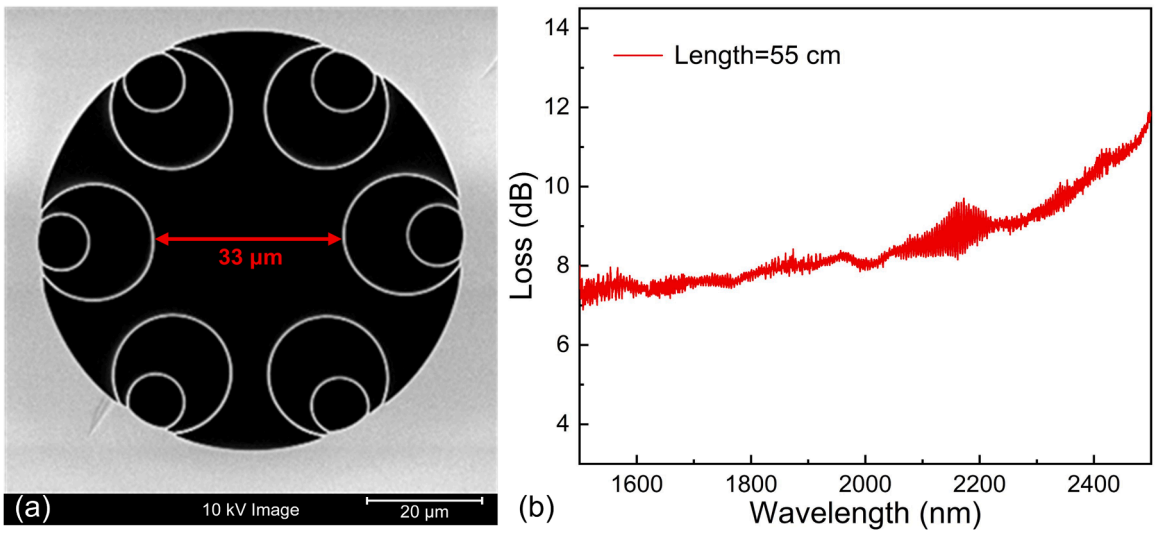

Fig. 1. (a) Cross section image of the used HC-ARF captured by the scanning electron microscope; (b) Transmission spectrum of the used HC-ARF.

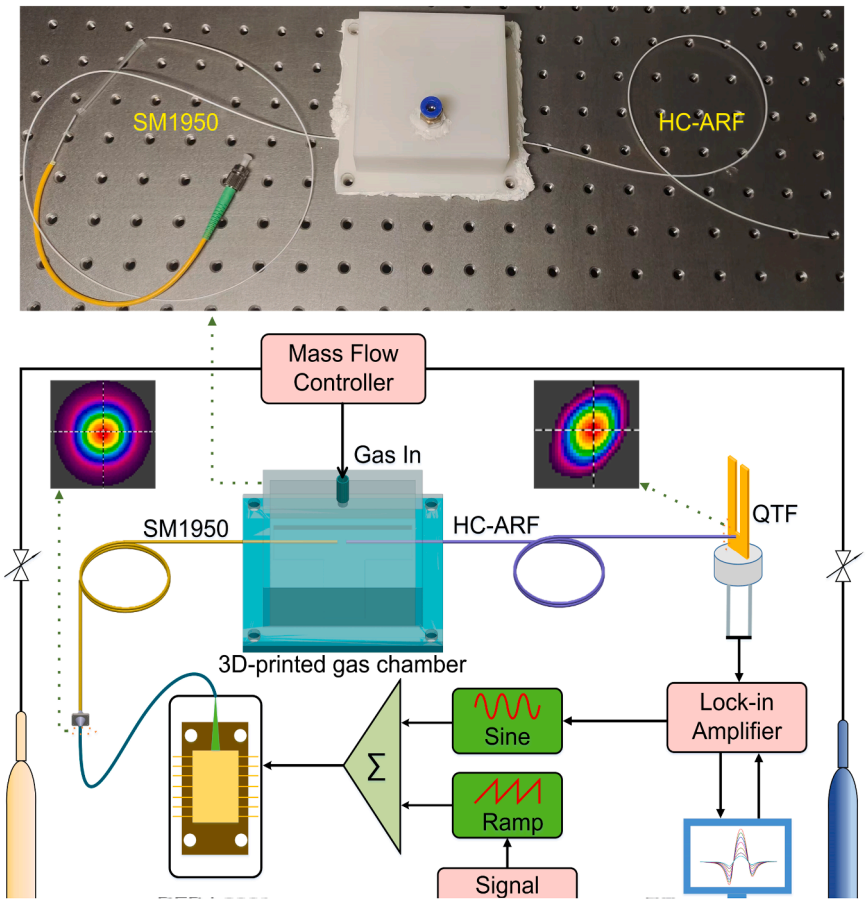

Fig. 2. The configuration of all-fiber LITES sensor based on HC-ARF.

3. Experimental results and discussion

Firstly, we investigated the resonance characteristics of the used QTF. The obtained experimental data were normalized and fitted with the Lorentz function and the generated frequency response curve is shown in Fig. 3. It can be find that the resonance frequency (f_0) and response bandwidth (Δf) were 32748.9 Hz and 3.03 Hz, respectively. Based on the formula for calculating the quality factor (Q) of QTF: $Q=f_0/\Delta f$, the calculated Q for used QTF in this study is 10808. This QTF has a high Q and narrow Δf, which means it has strong ability of energy accumulation and noise suppression.

In this experiment, due to the use of WMS and second harmonic demodulation techniques, the 2*f* signal level was related to the sine wave modulation amplitude. Therefore, the modulation depth of the system needs to be optimized. The values of the 2*f* signal at different modulation amplitudes were measured to acquire the optimum modulation depth. The obtained results are shown in Fig. 4. It can be seen that the 2*f* signal reached the maximum when the modulating current was 31.16 mA (4.29 GHz).

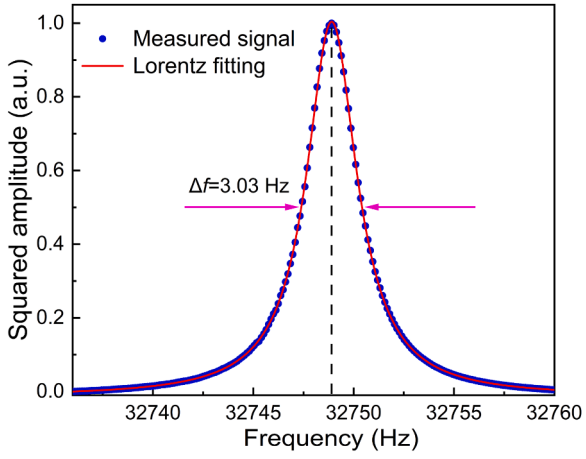

Fig. 3. Frequency response curve of the used QTF after normalisation and fitting with Lorentz function.

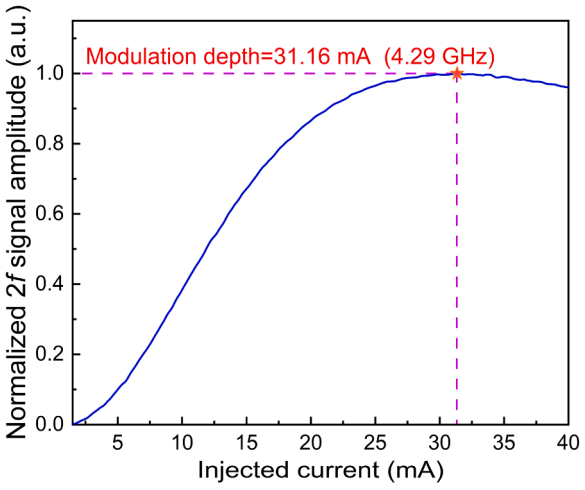

Fig. 4. The relationship between 2*f* signal amplitude and depth of modulation current.

The response speed of gas sensing system is determined by the filling time of the gas. The region of spatial coupling of SM1950 fiber and HC-ARF was placed in the gas chamber. In order to increase the pressure inside the gas chamber and facilitate the filling of the gas to be measured in the HC-ARF, the designed 3D-printed gas chamber was equipped with only an inlet port, and the end of the HC-ARF served as the outlet port. The air pressure level at the inlet was 780 Torr, and the air pressure at the fiber output end face was 760 Torr. Fig. 5 illustrates the curve of the 2*f* signal after the gas was changed from pure N_2 to 3% CO with a flow rate of of 120 mL/min. It can be seen that it took about 3 min for the gas to fill up the entire HC-ARF at this pressure, indicating a gas filling time of 3 min for this sensor.

The QTF had the maximum elastic deformation when the laser was directed to the central position of the QTF root. After this positon was determined, the relationship between the distance *Z* and the 2*f* signal value was optimized, where *Z* was the distance between the HC-ARF tip and the QTF surface, as shown in Fig. 6. It can be seen that as the distance *Z* increased, the 2*f* signal value decreased. This is due to the fact that the beam diameter increases with *Z*, resulting in a decrease in the power density of the incident spot at the root of the QTF, thereby affecting the 2*f* signal amplitude. When the distance *Z* was 0, the 2*f* signal had a maximum value. However, in order to avoid damaging the HC-ARF tip during the position adjustment procedure, the distance *Z* was adjusted as small as 0.05 mm because the 2*f* signal here was 98% of the maximum value and had little impact on system performance.

To verify the gas sensing performance of the all-fiber LITES sensor based on HC-ARF, different concentrations of CO was adopted. Fig. 7(a) demonstrates the 2*f* signals at different concentrations. The relationship between CO concentration and the 2*f* signal peak value is shown in Fig. 7 (b). After linear fitting, the expression $y = 0.0042x + 12.39$ was obtained, and the R-squared value was 0.99, indicating that the all-fiber LITES sensor based on HC-ARF had an excellent linear response to CO.

Subsequently, in order to obtain the minimum detection limit (MDL), pure N_2 was introduced into HC-ARF. The signal was continuously monitored for one minute, with a standard deviation (1σ) of 123.89 nV. By calculation, the MDL of the all-fiber LITES sensor based on HC-ARF was determined to be 27.53 ppm, resulting in a normalized noise equivalent absorption (NNEA) of 6.32×10^{-8} $cm^{-1}W{\cdot}Hz^{-1/2}$. Compared with the detection of CO using HC-ARF reported in reference [49], this work improved the MDL of CO by 61.9 times. In reference [44], fiber coupled multipass cell was used to detect CO, with an NNEA of 1.15×10^{-7} $cm^{-1}W{\cdot}Hz^{-1/2}$. It can be seen that by using an all-fiber structure instead of multipass cell, the detection performance of the system has been greatly improved. Finally, the long-term stability of the system was investigated. Pure N_2 was passed through the HC-ARF when the laser wavelength was set at the CO absorption line. The signal was

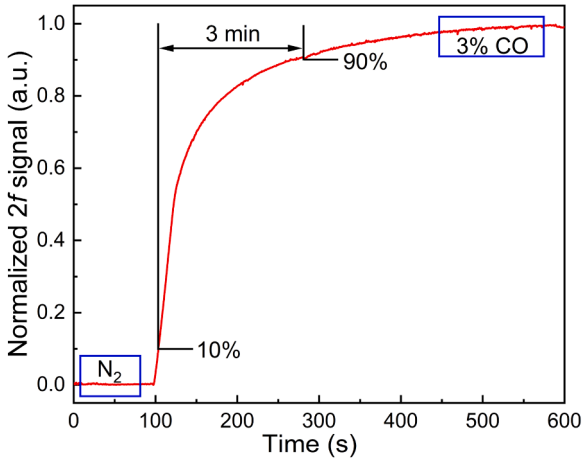

Fig. 5. Filling time of the all-fiber LITES sensor based on HC-ARF.

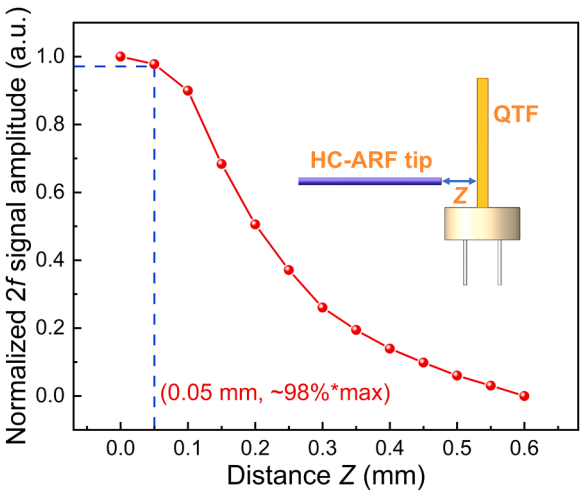

Fig. 6. The relationship between 2*f* signal amplitude and distance *Z*.

continuously monitored for more than 2.5 h, as shown in Fig. 8(a). Fig. 8 (b) shows the performance of the sensor without the laser on, which exhibits white noise for 2.5 h. The obtained data in Fig. 8(a) were analyzed by Allan deviation and the results are shown in Fig. 8(c). It can be seen that the MDL can reach 3.85 ppm at an averaging time of 100 s, which indicates that the all-fiber LITES sensor based on HC-ARF had good stability.

4. Conclusion

In conclusion, in order to overcome the limitations of large system size, multiple optical components and poor system stability in traditional LITES technique, a mid-infrared all-fiber LITES sensor based on a HC-ARF was reported for the first time. The all-fiber structure has advantages of low loss, easy optical alignment, good system stability, reduced sensor size and cost. The special circular structure in HC-ARF has a good suppression effect on mode interference noise. CO with an absorption line at 4291.50 cm^{-1} was chosen as the target gas to verify the sensing performance of the system in mid-infrared. The experimental results showed that the sensor had a good linear response to CO concentration, with a R-squared value of 0.99. The MDL of the all-fiber LITES sensor based on HC-ARF was determined as 27.53 ppm. Finally, the Allan deviation analysis demonstrated that the MDL of the system can reach 3.85 ppm at an average time of 100 s, indicating that the system had good long-term stability. In order to improve the detection performance of this mid-infrared all-fiber structure LITES sensor, a longer HC-ARF can be used in the future to increase the absorption length, or a CO fundamental absorption line can be chosen.

CRediT authorship contribution statement

Ma Yufei: Writing – review & editing, Supervision, Project administration, Conceptualization. **He Ying:** Methodology. **Zhu Jie:** Resources. **Chen Weipeng:** Writing – original draft, Investigation. **Qiao Shunda:** Validation. **Zhou Sheng:** Methodology. **Xiao Limin:** Resources. **Wang Kang:** Resources. **Qi Lei:** Validation, Funding acquisition.

Declaration of Competing Interest

The authors declare that they have no known competing financial interests or personal relationships that could have appeared to influence the work reported in this paper.

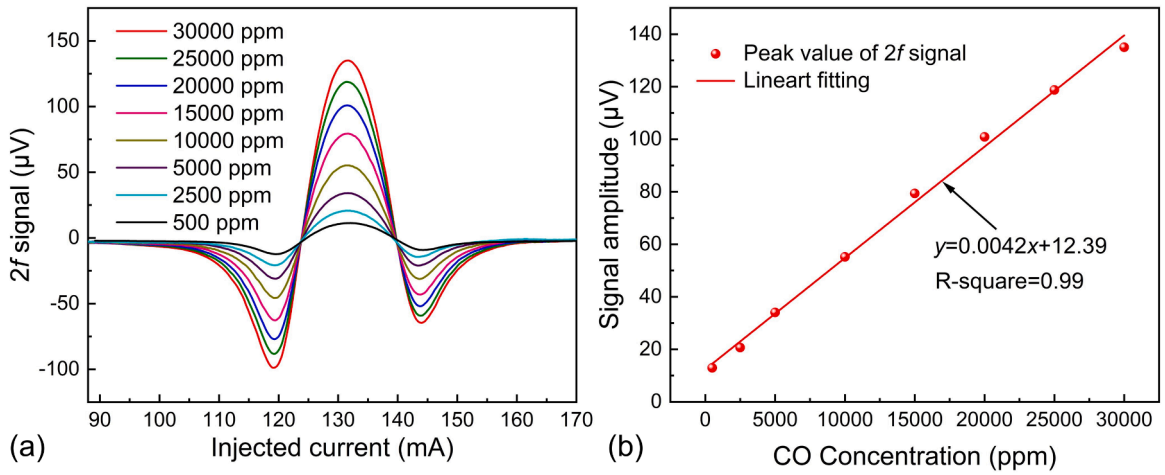

Fig. 7. (a) 2*f* signals at different CO concentrations; (b) The relationship between CO concentrations and corresponding 2*f* signal peak value.

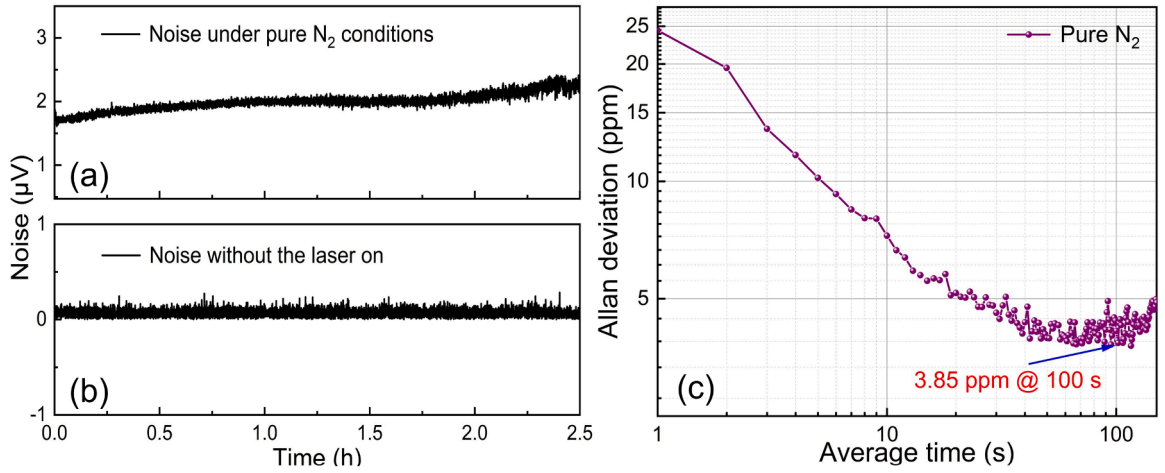

Fig. 8. (a) Continuous monitoring of noise for 2.5 h when introducing pure N_2; (b) Continuous monitoring of noise for 2.5 h without the laser on; (c) The results of Allan deviation analysis.

Data availability

Data will be made available on request.

Acknowledgments

We are grateful for financial supports from the National Natural Science Foundation of China (Grant No. 62335006, 62022032, 62275065, and 61875047), Key Laboratory of Opto-Electronic Information Acquisition and Manipulation (Anhui University), Ministry of Education (Grant No. OEIAM202202), Fundamental Research Funds for the Central Universities (Grant No. HIT.OCEF.2023011).

References

[1] A. Li, C. Wang, F.X. Bao, W.J. Fang, Y.X. Liang, R. Cheng, S.L. Pan, An integrated single-shot spectrometer with large bandwidth-resolution ratio and wide operation temperature range, PhotoniX 4 (1) (2023) 29.
[2] G.Y. Chen, Y.B. Sun, P.C. Shi, T. Liu, Z.H. Li, S.H. Luo, X.C. Wang, X.Y. Cao, B. Ren, G.K. Liu, Revealing unconventional host–guest complexation at nanostructured interface by surface-enhanced Raman spectroscopy, Light Sci. Appl. 10 (1) (2021) 85.
[3] C. Zhang, S. Qiao, Y. He, Y. Ma, Trace gas sensor based on a multi-pass-retro-reflection-enhanced differential Helmholtz photoacoustic cell and a power amplified diode laser, Opt. Express 32 (1) (2024) 848–856.
[4] H.J. Luo, Z.F. Yang, R.B. Zhuang, H.H. Lv, C.L. Wang, H.Y. Lin, D. Zhang, W. G. Zhu, Y.C. Zhong, Y. Cao, K. Liu, R.F. Kan, Y.W. Pan, J.H. Yu, H.D. Zheng, Ppbv-level mid-infrared photoacoustic sensor for mouth alcohol test after consuming lychee fruits, Photoacoustics 33 (2023) 100559.
[5] L. Wu, X. Yuan, Y. Tang, S. Wageh, O.A. Al-Hartomy, A.G. Al-Sehemi, J. Yang, Y. Xiang, H. Zhang, Y. Qin, MXene sensors based on optical and electrical sensing signals: from biological, chemical, and physical sensing to emerging intelligent and bionic devices, PhotoniX 4 (2023) 15.
[6] Y.F. Ma, R. Lewicki, M. Razeghi, F.K. Tittel, QEPAS based ppb-level detection of CO and N_2O using a high power CW DFB-QCL, Opt. Express 21 (1) (2013) 1008–1019.
[7] Z.D. Zhang, T. Peng, X.Y. Nie, G.S. Agarwal, M.O. Scully, Entangled photons enabled time-frequency-resolved coherent Raman spectroscopy and applications to electronic coherences at femtosecond scale, Light Sci. Appl. 11 (1) (2022) 274.
[8] W. Chen, S. Qiao, Z. Zhao, S. Gao, Y. Wang, Y. Ma, Sensitive carbon monoxide detection based on laser absorption spectroscopy with hollow-core antiresonant fiber, Microw. Opt. Techn. Lett. 66 (1) (2024) e33780.
[9] Y. Liu, S. Qiao, C. Fang, Y. He, H. Sun, J. Liu, Y. Ma, A highly sensitive LITES sensor based on a multi-pass cell with dense spot pattern and a novel quartz tuning fork with low frequency, Opto-Electron. Adv. 7 (2024) 230230, https://doi.org/10.29026/oea.2024.230230.
[10] T. Liang, S. Qiao, Y. Chen, Y. He, Y. Ma, High-sensitivity methane detection based on QEPAS and H-QEPAS technologies combined with a self-designed 8.7 kHz quartz tuning fork, Photoacoustics 36 (2024) 100592.
[11] Y.H. Liu, Y.F. Ma, Advances in multipass cell for absorption spectroscopy-based trace gas sensing technology, Chin. Opt. Lett. 21 (3) (2023) 033001.
[12] H. Wang, Z. Zhan, F. Hu, Y. Meng, Z. Liu, X. Fu, Q. Liu, Intelligent optoelectronic processor for orbital angular momentum spectrum measurement, PhotoniX 4 (2023) 9.
[13] A. Leal-Junior, L. Avellar, V. Biazi, M.S. Soares, A. Frizera, C. Marques, Multifunctional flexible optical waveguide sensor: on the bioinspiration for ultrasensitive sensors development, Opto-Electron. Adv. 5 (10) (2022) 210098.
[14] M. Yan, P.L. Luo, K. Iwakuni, G. Millot, T.W. Hänsch, N. Picqué, Mid-infrared dual-comb spectroscopy with electro-optic modulators, Light Sci. Appl. 6 (10) (2017) e17076.

[15] B.X. Xu, X.Y. Fan, S. Wang, Z.Y. He, Sub-femtometer-resolution absolute spectroscopy with sweeping electro-optic combs, Opto-Electron. Adv. 5 (12) (2022) 210023.
[16] T. Wang, J.F. Jiang, K. Liu, S. Wang, P.P. Niu, Y.Z. Liu, T.G. Liu, Flexible minimally invasive coherent anti-Stokes Raman spectroscopy (CARS) measurement method with tapered optical fiber probe for single-cell application, PhotoniX 3 (1) (2022) 11.
[17] W. Yang, F. Knorr, I. Latka, M. Vogt, G.O. Hofmann, J. Popp, I.W. Schie, Real-time molecular imaging of near-surface tissue using Raman spectroscopy, Light Sci. Appl. 11 (1) (2022) 90.
[18] Y.Q. Wang, J.H. Zhang, Y.C. Zheng, Y.R. Xu, J.Q. Xu, J. Jiao, Y. Su, H.F. Lü, K. Liang, Brillouin scattering spectrum for liquid detection and applications in oceanography, Opto-Electron. Adv. 6 (1) (2023) 220016.
[19] C. Zhang, Y. He, S.D. Qiao, Y.F. Ma, Differential integrating sphere-based photoacoustic spectroscopy gas sensing, Opt. Lett. 48 (19) (2023) 5089–5092.
[20] Y.F. Qi, Y.H. Liu, J.B. Luo, Recent application of Raman spectroscopy in tumor diagnosis: from conventional methods to artificial intelligence fusion, PhotoniX 4 (1) (2023) 22.
[21] P.P. Shum, G. Keiser, G. Humbert, D.J.J. Hu, A.P. Zhang, L. Su, Highly sensitive microfiber ultrasound sensor for photoacoustic imaging, Opto-Electron. Adv. 6 (6) (2023) 230065.
[22] Y.F. Wang, H.Y. Du, Y.Q. Li, F. Mei, Y. Hu, L.T. Xiao, J. Ma, S.T. Jia, Testing universality of Feynman-Tan relation in interacting Bose gases using high-order Bragg spectra, Light Sci. Appl. 12 (1) (2023) 50.
[23] A.A. Kosterev, Y.A. Bakhirkin, R.F. Curl, F.K. Tittel, Quartz-enhanced photoacoustic spectroscopy, Opt. Lett. 27 (21) (2002) 1902–1904.
[24] Z.J. Shang, S.Z. Li, B. Li, H.P. Wu, A. Sampaolo, P. Patimisco, V. Spagnolo, L. Dong, Quartz-enhanced photoacoustic NH_3 sensor exploiting a large-prong-spacing quartz tuning fork and an optical fiber amplifier for biomedical applications, Photoacoustics 26 (2022) 100363.
[25] C. Zhang, S.D. Qiao, Y. He, S. Zhou, L. Qi, Y.F. Ma, Differential quartz-enhanced photoacoustic spectroscopy, Appl. Phys. Lett. 122 (24) (2023) 241103.
[26] Z.T. Lang, S.D. Qiao, T.T. Liang, Y. He, L. Qi, Y.F. Ma, Dual-frequency modulated heterodyne quartz-enhanced photoacoustic spectroscopy, Opt. Express 32 (1) (2024) 379–386.
[27] C. Fang, T. Liang, S. Qiao, Y. He, Z. Shen, Y. Ma, Quartz-enhanced photoacoustic spectroscopy sensing using trapezoidal- and round-head quartz tuning forks, Opt. Lett. 49 (3) (2024) 770–773.
[28] L.E. Hu, C.T. Zheng, M.H. Zhang, D. Yao, J. Zheng, Y. Zhang, Y.D. Wang, F. K. Tittel, Quartz-enhanced photoacoustic spectroscopic methane sensor system using a quartz tuning fork-embedded, double-pass and off-beam configuration, Photoacoustics 18 (2020) 100174.
[29] G. Menduni, A. Zifarelli, A. Sampaolo, P. Patimisco, M. Giglio, N. Amoroso, H. Wu, L. Dong, R. Bellotti, V. Spagnolo, High-concentration methane and ethane QEPAS detection employing partial least squares regression to filter out energy relaxation dependence on gas matrix composition, Photoacoustics 26 (2022) 100349.
[30] C. Fang, S.D. Qiao, Y. He, Z.C. Shen, Y.F. Ma, Design and sensing performance of T-shaped quartz tuning forks, Acta Opt. Sin. 43 (18) (2023) 1899910.
[31] Z. Lang, S. Qiao, Y. He, Y. Ma, Quartz tuning fork-based demodulation of an acoustic signal induced by photo-thermo-elastic energy conversion, Photoacoustics 22 (2021) 100272.
[32] Y.F. Ma, Y. He, X. Yu, C. Chen, R. Sun, F.K. Tittel, HCl ppb-level detection based on QEPAS sensor using a low resonance frequency quartz tuning fork, Sens. Actuat. B-Chem. 233 (2016) 388–393.
[33] Y. He, Y.F. Ma, Y. Tong, X. Yu, F.K. Tittel, HCN ppt-level detection based on a QEPAS sensor with amplified laser and a miniaturized 3D-printed photoacoustic detection channel, Opt. Express 26 (8) (2018) 9666–9675.
[34] Y.F. Ma, Y. He, Y. Tong, X. Yu, F.K. Tittel, Quartz-tuning-fork enhanced photothermal spectroscopy for ultra-high sensitive trace gas detection, Opt. Express 26 (24) (2018) 32103–32110.
[35] W.P. Chen, S.D. Qiao, Z.T. Lang, J.C. Jiang, Y. He, Y.W. Shi, Y.F. Ma, Hollow-waveguide-based light-induced thermoelastic spectroscopy sensing, Opt. Lett. 48 (15) (2023) 3989–3992.
[36] B. Sun, P. Patimisco, A. Sampaolo, A. Zifarelli, V. Spagnolo, H.P. Wu, L. Dong, Light-induced thermoelastic sensor for ppb-level H_2S detection in a SF_6 gas matrices exploiting a mini-multi-pass cell and quartz tuning fork photodetector, Photoacoustics 33 (2023) 100553.
[37] X.N. Liu, Y.F. Ma, New temperature measurement method based on light-induced thermoelastic spectroscopy, Opt. Lett. 48 (21) (2023) 5687–5690.
[38] Z.T. Lang, S.D. Qiao, Y.F. Ma, Fabry–Perot-based phase demodulation of heterodyne light-induced thermoelastic spectroscopy, Light Adv. Manuf. 4 (2023) 23.
[39] Y.F. Ma, T.T. Liang, S.D. Qiao, X.N. Liu, Z.T. Lang, Highly Sensitive and fast hydrogen detection based on light-induced thermoelastic spectroscopy, Ultrafast. Sci. 3 (2023) 0024.
[40] S. Qiao, Y. Ma, Y. He, P. Patimisco, A. Sampaolo, V. Spagnolo, Ppt level carbon monoxide detection based on light-induced thermoelastic spectroscopy exploring custom quartz tuning forks and a mid-infrared QCL, Opt. Express 29 (16) (2021) 25100–25108.
[41] C.G. Lou, X.T. Li, H.J. Chen, X. Yang, Y. Zhang, J.Q. Yao, X.L. Liu, Polymer-coated quartz tuning fork for enhancing sensitivity of laser-induced thermoelastic spectroscopy, Opt. Express 29 (8) (2021) 12195–12205.
[42] Y.F. Ma, Y. He, P. Patimisco, A. Sampaolo, S.D. Qiao, X. Yu, F.K. Tittel, V. Spagnolo, Ultra-high sensitive trace gas detection based on light-induced thermoelastic spectroscopy and a custom quartz tuning fork, Appl. Phys. Lett. 116 (1) (2020) 011103.
[43] S.D. Qiao, P.Z. Ma, V. Tsepelin, G.W. Han, J.X. Liang, W. Ren, H.D. Zheng, Y.F. Ma, Super tiny quartz-tuning-fork-based light-induced thermoelastic spectroscopy sensing, Opt. Lett. 48 (2) (2023) 419–422.
[44] X.N. Liu, Y.F. Ma, Sensitive carbon monoxide detection based on light-induced thermoelastic spectroscopy with a fiber-coupled multipass cell, Chin. Opt. Lett. 20 (3) (2022) 031201.
[45] Y. He, Y.F. Ma, Y. Tong, X. Yu, F.K. Tittel, Ultra-high sensitive light-induced thermoelastic spectroscopy sensor with a high Q-factor quartz tuning fork and a multipass cell, Opt. Lett. 44 (8) (2019) 1904–1907.
[46] L.E. Hu, C.T. Zheng, Y. Zhang, J. Zheng, Y.D. Wang, F.K. Tittel, Compact all-fiber light-induced thermoelastic spectroscopy for gas sensing, Opt. Lett. 45 (7) (2020) 1894–1897.
[47] Y.F. Ma, Y. Tong, Y. He, X.G. Jin, F.K. Tittel, Compact and sensitive mid-infrared all-fiber quartz-enhanced photoacoustic spectroscopy sensor for carbon monoxide detection, Opt. Express 27 (6) (2019) 9302–9312.
[48] S.M. Mejia Quintero, L.C. Guedes Valente, M.S. de Paula Gomes, H. Gomes da Silva, B. Caroli de Souza, S.R.K. Morikawa, All-Fiber CO_2 Sensor Using Hollow Core PCF Operating in the 2 μm Region, Sensors 18 (12) (2018) 4393.
[49] Y.F. Ma, W. Feng, S.D. Qiao, Z.X. Zhao, S.F. Gao, Y.Y. Wang, Hollow-core anti-resonant fiber based light-induced thermoelastic spectroscopy for gas sensing, Opt. Express 30 (11) (2022) 18836–18844.
[50] G. Gomółka, D. Pysz, R. Buczyński, M. Nikodem, Wavelength modulation spectroscopy of oxygen inside anti-resonant hollow-core fiber-based gas cell, Opt. Laser Technol. 170 (2024) 110323.
[51] P. Bojęś, P. Jaworski, P. Pokryszka, W. Belardi, V. Spagnolo, K. Krzempek, Dual-band light-induced thermoelastic spectroscopy utilizing an antiresonant hollow-core fiber-based gas absorption cell, Appl. Phys. B 129 (11) (2023) 177.
[52] S.L. Jiang, F.F. Chen, Y. Zhao, S.F. Gao, Y.Y. Wang, H.L. Ho, W. Jin, Broadband all-fiber optical phase modulator based on photo-thermal effect in a gas-filled hollow-core fiber, Opto-Electron. Adv. 6 (5) (2023) 220085.
[53] C.Y. Wang, R.W. Yu, B. Debord, F. Gérôme, F. Benabid, K.S. Chiang, L.M. Xiao, Ultralow-loss fusion splicing between negative curvature hollow-core fibers and conventional SMFs with a reverse-tapering method, Opt. Express 29 (14) (2021) 22470–22478.
[54] R.W. Yu, C.Y. Wang, F. Benabid, K.S. Chiang, L.M. Xiao, Robust mode matching between structurally dissimilar optical fiber waveguides, ACS Photonics 8 (3) (2021) 857–863.

Weipeng Chen received his B.S. degree in electronic science and technology from Yanshan university, China, in 2022. In the same year he pursued a master's degree in physical electronics from Harbin Institute of Technology. His research interest is focused on light-induced thermoelastic spectroscopy.

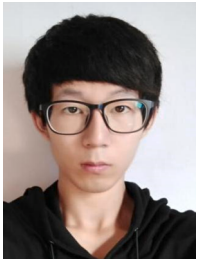

Shunda Qiao received his B.S. degree in electronic science and technology from Yanshan university, China, in 2018. In 2020, he received his M.S. degree and began to pursue a PhD degree of physical electronics from Harbin Institute of Technology. His research interests include photoacoustic spectroscopy and its applications.

Ying He obtained his master and doctorate degrees in physical electronics from Harbin Institute of Technology in 2017 and 2022, respectively. Currently, he is an associate professor at the Harbin Institute of Technology, China. His research interests including trace gas sensing based on QEPAS, LITES and other laser spectroscopy.

Jie Zhu received the master's degree in Northwestern Polytechnical University, Xi'an, China. He is currently working toward the Ph.D. degree in optical engineering at Fudan University, Shanghai, China. His research interests include anti-resonant hollow-core fiber manufacturing technology, all-fiber devices and fiber sensors.

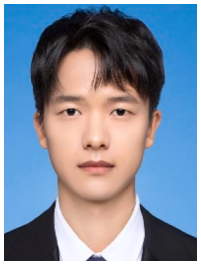

Kang Wang received his bachelor's degree in electronic science and technology from Shandong University in 2021. He is currently pursuing the master's degree in optical engineering from Fudan University. His main research area is fiber sensors.

Lei Qi was born in Weifang, Shandong, PRC, on Oct 22, 1985. He received a Ph.D. degree in 2020 from Tianjin University. From 2012 to 2018, he was an engineer at Beijing Institute of Spacecraft Environment Engineering. From 2018, He serves as a senior engineer at Beijing Institute of Spacecraft Environment Engineering.

Sheng Zhou received his PhD degree in the Institute of Optics and Electronics, Chinese Academy of Sciences (CAS), China. Now, he has been an associate professor of the Key Laboratory of Opto-Electronic Information Acquisition and Manipulation of Ministry of Education. His research focuses on the fields of high sensitive cavity ring-down spectroscopy techniques for exhaled breath biomarkers analysis, atmospheric trace species monitoring and industrial process control.

Limin Xiao received his Ph.D. from the Hong Kong Polytechnic University. He is currently a Professor with the Key Laboratory of Micro and Nano Photonic Structures, Fudan University, Shanghai, China. He is also with the Key Laboratory for Information Science of Electromagnetic Waves (MoE), Fudan University, and also with Shanghai Engineering Research Center of Ultra-Precision Optical Manufacturing, Fudan University. He currently heads the Advanced Fiber Devices and Systems Group. His research interests include photonic crystal fibers and devices, advanced optical fiber manufacturing technology, fiber sensors, all-fiber devices, and laser technology.

Yufei Ma received his PhD degree in physical electronics from Harbin Institute of Technology, China, in 2013. From September 2010 to September 2011, he spent as a visiting scholar at Rice University, USA. Currently, he is a professor at Harbin Institute of Technology, China. He is the winner of National Outstanding Youth Science Fund. His research interests include optical sensors, trace gas detection, laser spectroscopy, solid-state laser and optoelectronics. He has published more than 100 publications and given more than 20 invited presentations at international conferences. He serves as associate editor for Optica *Optics Express*, SPIE *Optical Engineering*, Wiley *Microwave and Optical Technology Letters* and *Frontiers in Physics*. He also serves as topical editor for CLP *Chinese Optics Letters* and editorial board member for Elsevier *Photoacoustics* MDPI *Sensors* and *Applied Sciences*.